Supplement of

Critical Load Exceedances for North America and Europe using an Ensemble of Models and an Investigation of Causes for Environmental Impact Estimate Variability: An AQMEII4 Study

Paul A. Makar et al.

Correspondence to : Paul A. Makar (paul.makar@ec.gc.ca)

This PDF file includes the following information:

1.0 Background information – Introduction to the Critical Load concept 1

2.0 Critical Load Exceedance Maps for Europe, 2009, and North America, 2010. 3

3.0 Observation Station Locations 10

4.0 Cross-track Infrared Sounding (CrIS) Sensor Retrieval Details 13

5.0 Precipitation Evaluation 14

6.0 Additional annual effective mass flux figures 15

1.0 Background information – Introduction to the Critical Load concept

As noted in the main document, a critical load in this context was defined (Nilsson and Grennfelt, 1988) as "A quantitative estimate of an exposure to one or more pollutants below which significant harmful effects on specified sensitive elements of the environment do not occur, according to present knowledge".

The Nilsson and Grennfelt (1988) definition is worthy of parsing in order to ensure understanding of its implications in context to the present work, and doing so will aid in the interpretation of our analysis results.

With regards to "exposure to one or more pollutants", both sulphur and nitrogen-containing compounds are considered to be relevant for acidification, and these may be deposited in different forms. Sulphur is deposited as gaseous sulphur dioxide (SO_2 dry deposition), as sulphate or bisulphite ions in precipitation (SO_4^{2-} and HSO_3^- wet deposition), or when particles containing sulphate reach and remain on the surface (particulate sulphate dry deposition). Nitrogen deposition comprises a larger number of chemical species, with contributions of dry deposition of gases (nitrogen dioxide (NO_2), nitric acid (HNO_3), ammonia (NH_3), peroxyacetylnitrate (PAN), organic nitrates (a host of possible species), dinitrogen pentoxide (N_2O_5), pernitric acid (HNO_4) and nitrogen monoxide (NO), and a variety of other species in low concentrations), nitrate and ammonium ions in precipitation (NO_3^- and NH_4^+ wet deposition), and dry deposition of particulate nitrate and ammonium. Chemical transport models (CTMs) must therefore accurately estimate the sulphur and nitrogen containing species' emissions, transport, chemical reactions (gaseous, particulate, aqueous), cloud processing (uptake of gases and aerosols into hydrometeors such as cloud water, rain, snow, graupel, etc), precipitation (transfer of the resulting chemically transformed species to the surface of the earth during precipitation events), and removal fluxes at the surface (dry deposition). The manner in which these complex processes are carried out depends on the implementation details of the specific CTM. As atmospheric science progresses, the process representation of the CTMs changes and improves. Estimates of environmental impacts of deposition may thus also change over time, not just in response to changes in emissions and other atmospheric and environmental conditions, but also due to the gradual progress of air-quality modelling science.

With regards to "according to present knowledge" – this part of the definition also acknowledges that knowledge changes over time. The underlying data used in estimating critical loads may improve – for example by including chemical species previously believed to have an insignificant impact on exceedances (Liggio *et al.*, 2024). The CTMs used to generate deposition fluxes for critical load development and critical load exceedance (CLE) estimates are frequently updated, with new process representation, which in turn may lead to changes in the predicted deposition fluxes. The emissions inputs to the models may also change, reflecting better emissions data collection, the enactment of emissions control legislation, changing environmental conditions (year to year variability in meteorology, as well as climate change), and changes in the quality of land use and proxy data used to determine both emissions and deposition fluxes. These changes imply the need to carry out critical load exceedance calculations on an ongoing basis, so that the estimation of ecosystem impact assessments makes use of the most recent science and best available input data.

With regards to "below which *significant* harmful effects on specified sensitive elements of the environment do *not* occur,": the usual approach in defining critical loads is to set, in advance, a level of ecosystem change that is expected to have negative effects on connected components or ecosystem services. Typically, the pollutant loading corresponding to a certain level of ecosystem damage is used (e.g., the amount of acidifying deposition at which 90 or 95% of sensitive species remain undamaged despite the given deposition level, the amount of N deposition resulting in 80% of sensitive plant species remaining undamaged, etc.; CLRTAP, 2023). Critical load values vary across the landscape and ecosystem components. For example, lichen communities are very sensitive to small changes, while herbaceous communities have natural buffers that require higher levels of deposition before species are lost (Simkin *et al.,* 2016, Geiser *et al.,* 2019). Potential ecosystem damage is considered to be "significant" above this level of deposition – but deposition below the critical load does not imply an *absence* of potential ecosystem damage.

References:

CLRTAP, 2023: UNECE CLRTAP (2023). Manual on Methodologies and Criteria for Modelling and Mapping Critical Loads and Levels and Air Pollution Effects, Risks, and Trends. Dessau-Roßlau, UBA TEXTE 109/2023. https://www.umweltbundesamt.de/en/publikationen/manual-on-methodologies-criteria-for-modelling-0

Geiser, L. H., Nelson, P.R., Jovan, S.E., Root, H.T., and Clark, C.M., Assessing Ecological Risks from Atmospheric Deposition of Nitrogen and Sulfur to US Forests Using Epiphytic Macrolichens, Diversity 11(6): 87, 2019. https://doi.org/10.3390/d11060087

Liggio, J., Makar, P.A., Li, S-M., Hayden, K., Darlington, A., Moussa, S., Wren, S., Staebler, R., Wentzell, J., Wheeler, M., Leithead, A., Mittermeier, R., Narayan, J., Wolde, M., Blanchard, D., Aherne, J., Kirk, J., Lee, C., Stroud, C., Zhang, J., Akingunola, A., Katal, A., Cheung, P., Ghahreman, R., Majdzadeh, M., He, M., Ditto, J., Gentner, D.R., Total organic carbon dry deposition outpaces atmospheric processing with unaccounted implications for air quality and freshwater ecosystems, Science Advances, (under review), 2024.

Nilsson, J., and Grennfelt, P., Critical loads for sulphur and nitrogen, in: Report from a workshop held at Skokloster, Sweden 19–24 March 1988, J. Nilsson, Ed., Miljorapport, Volume 15 of Nordic Council of Ministers-Publications-Nord, 418pp, 1988. Simkin *et al.*, 2016

Simkin, S. M., Allen, E.B., Bowman, W.D., Clark, C.M., Belnap, J., Brooks, M.L., Cade, B.S., Collins, S.L., Geiser, L.H., Gilliam, F.S., Jovan, S.E., Pardo, L.H., Schulz, B.K., Stevens, C.I., Suding, K.N., Throop, H.L., and Waller, D.M., Conditional vulnerability of plant diversity to atmospheric nitrogen deposition across the United States, Proc. Nat. Acad. Sci., 113(15), 4086-4091, 2016. https://doi.org/10.1073/pnas.1515241113

2.0 Critical Load Exceedance Maps for Europe, 2009, and North America, 2010.

Figure S1. CLEs for Acidity, EU domain, 2009, eq $ha^{-1}yr^{-1}$ (a) WRF-Chem (IASS), (b) LOTOS-EUROS (TNO), (c) WRF-Chem (UPM), (d) CMAQ (Hertfordshire). Grey areas indicate regions for which critical load data are available but are not in exceedance of critical loads. Coloured areas indicate exceedance regions.

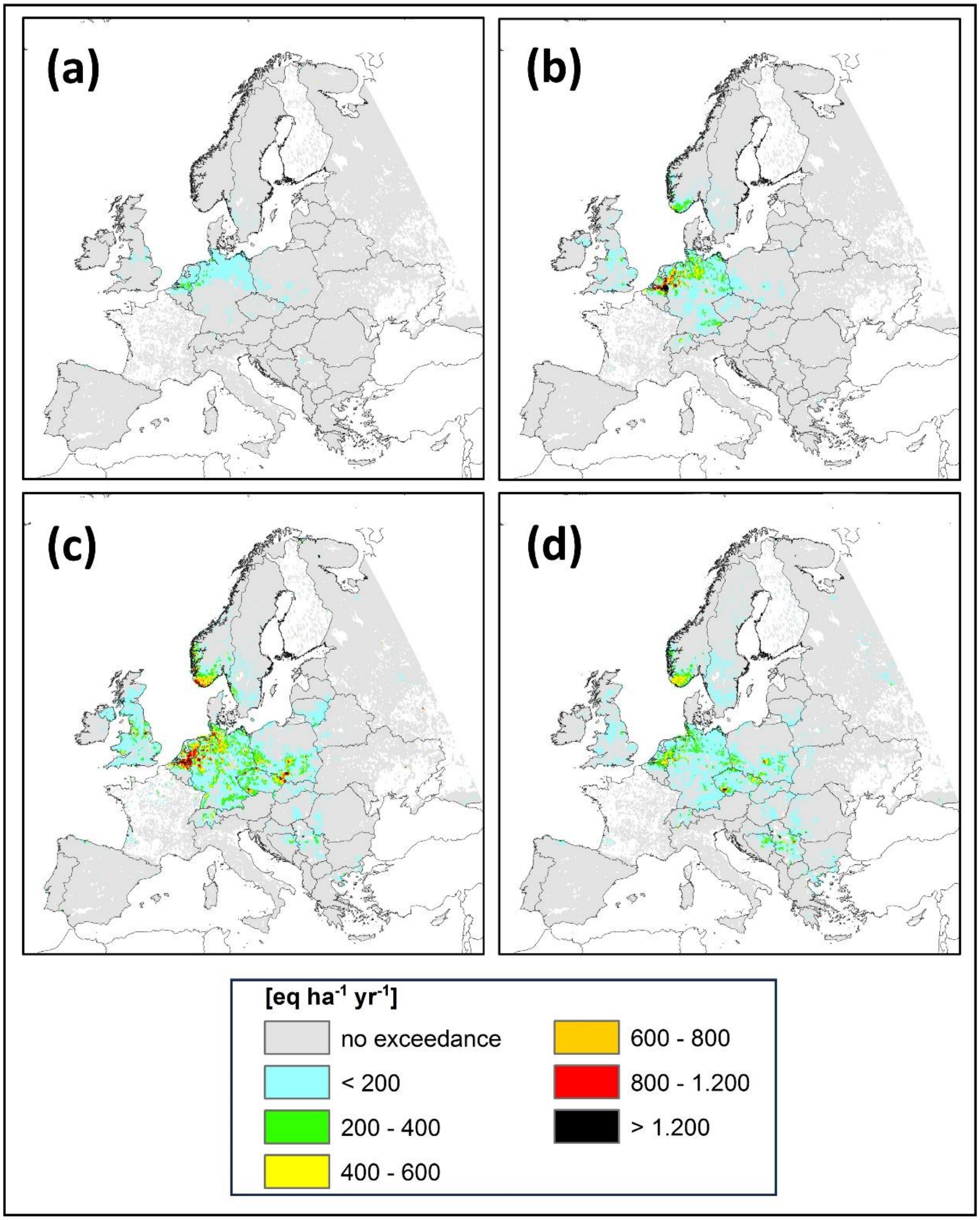

Figure S2. CLEs for Eutrophication, EU domain, 2009, eq ha^{-1}yr^{-1} (a) WRF-Chem (IASS), (b) LOTOS-EUROS (TNO), (c) WRF-Chem (UPM), (d) CMAQ (Hertfordshire). Grey areas indicate regions for which critical load data are available but are not in exceedance of critical loads. Coloured areas indicate exceedance regions.

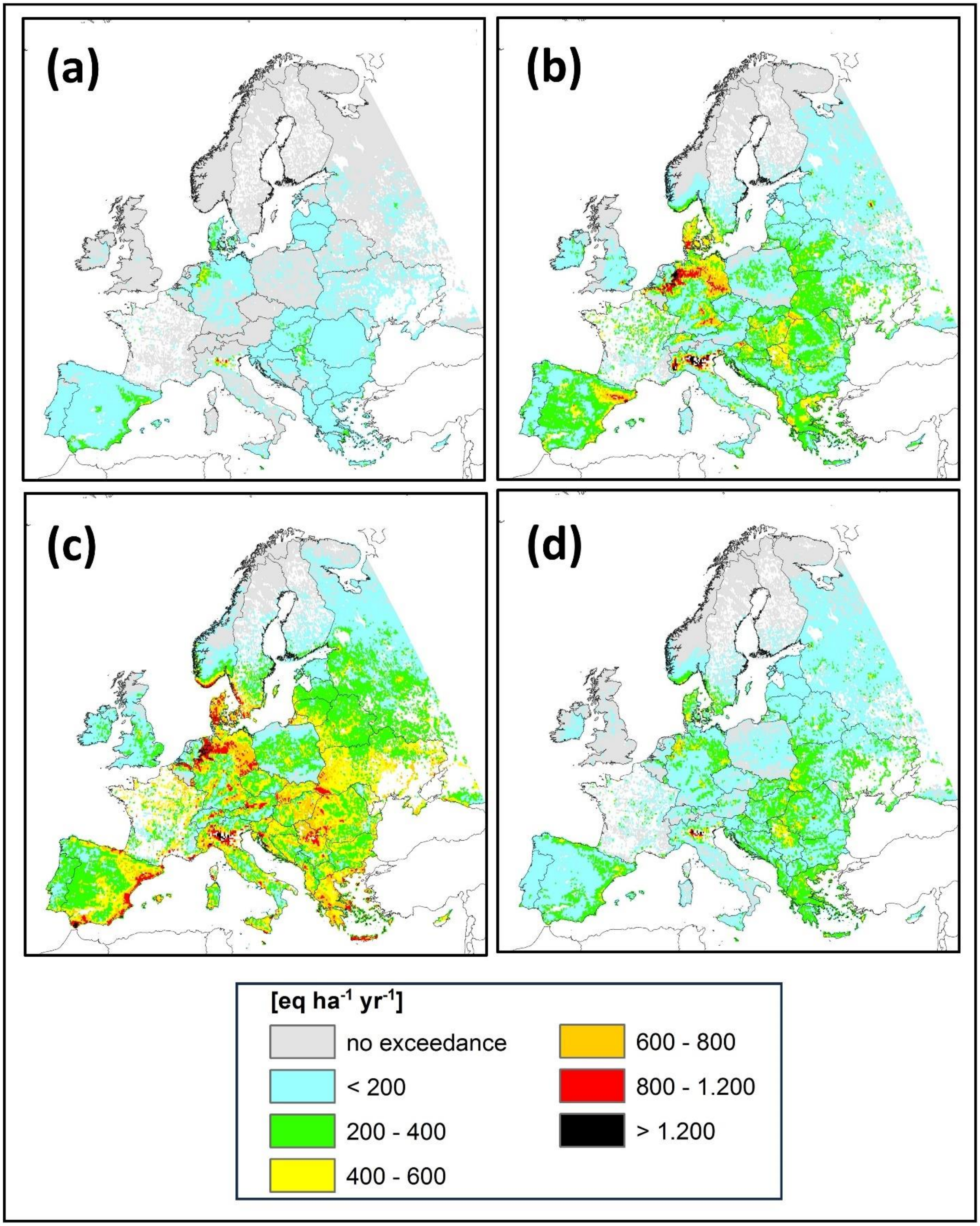

Figure S3. CLEs for Forest Ecosystems, NA domain, 2010, eq $ha^{-1}yr^{-1}$ (a) CMAQ-M3DRY (EPA), (b) CMAQ-STAGE (EPA), (c) WRF-Chem (IASS), (d) GEM-MACH-Base (ECCC), (e) GEM-MACH-Zhang (ECCC), (f) GEM-MACH-Ops (ECCC), (g) WRF-Chem (UPM), (h) WRF-Chem (UCAR). Grey areas indicate regions for which critical load data are available but are not in exceedance of critical loads. Coloured areas indicate exceedance regions.

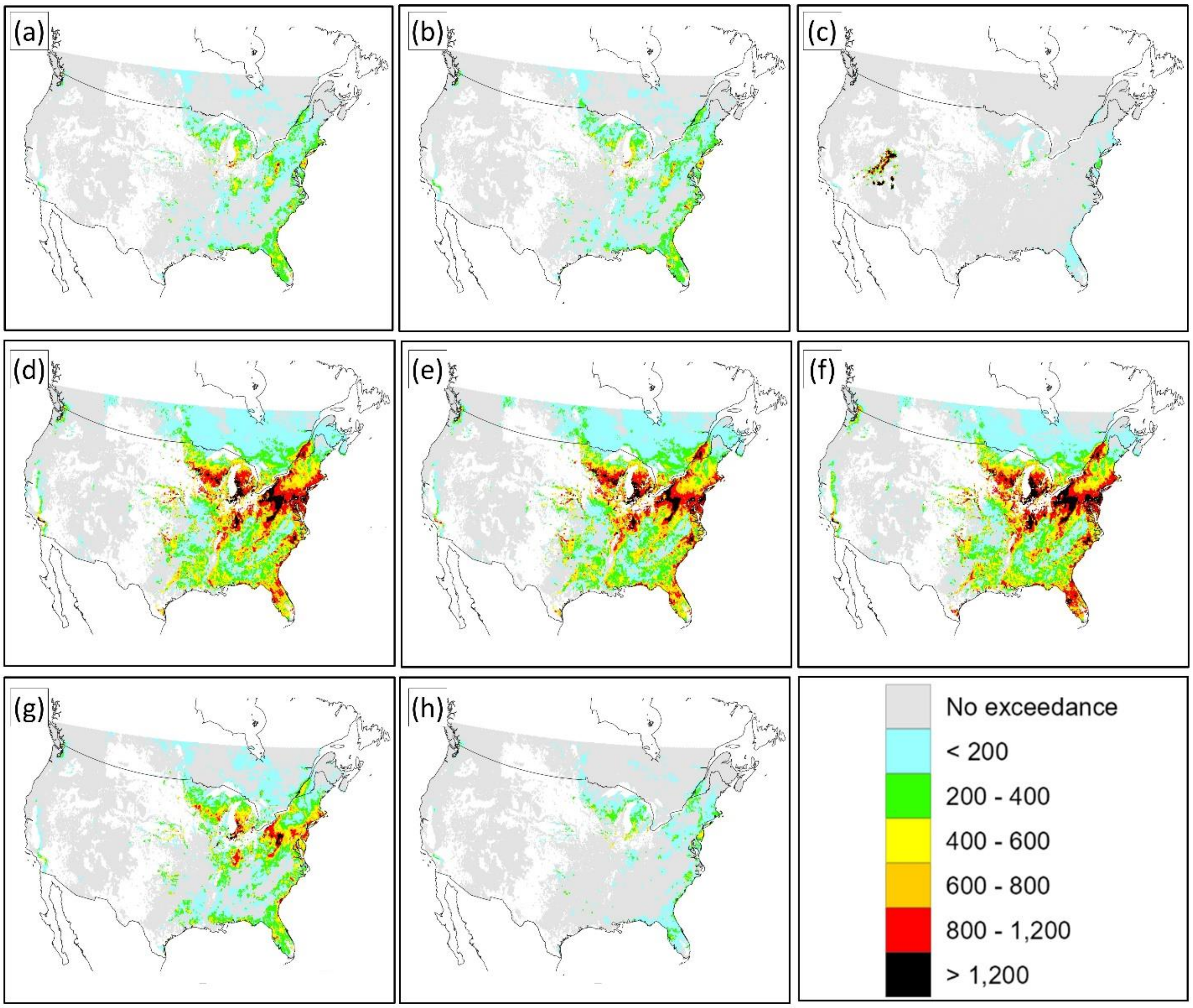

Figure S4. CLEs for Aquatic Ecosystems, NA domain, 2010, eq ha^{-1}yr^{-1}. Panels arranged as in Figure S3; individual lakes are shown as pixels. Light grey pixels indicate regions for which critical load data were available but were not in exceedance of critical loads. Coloured areas indicate exceedance regions; overplotting in precedence by the extent of exceedance was carried out for overlapping pixels.

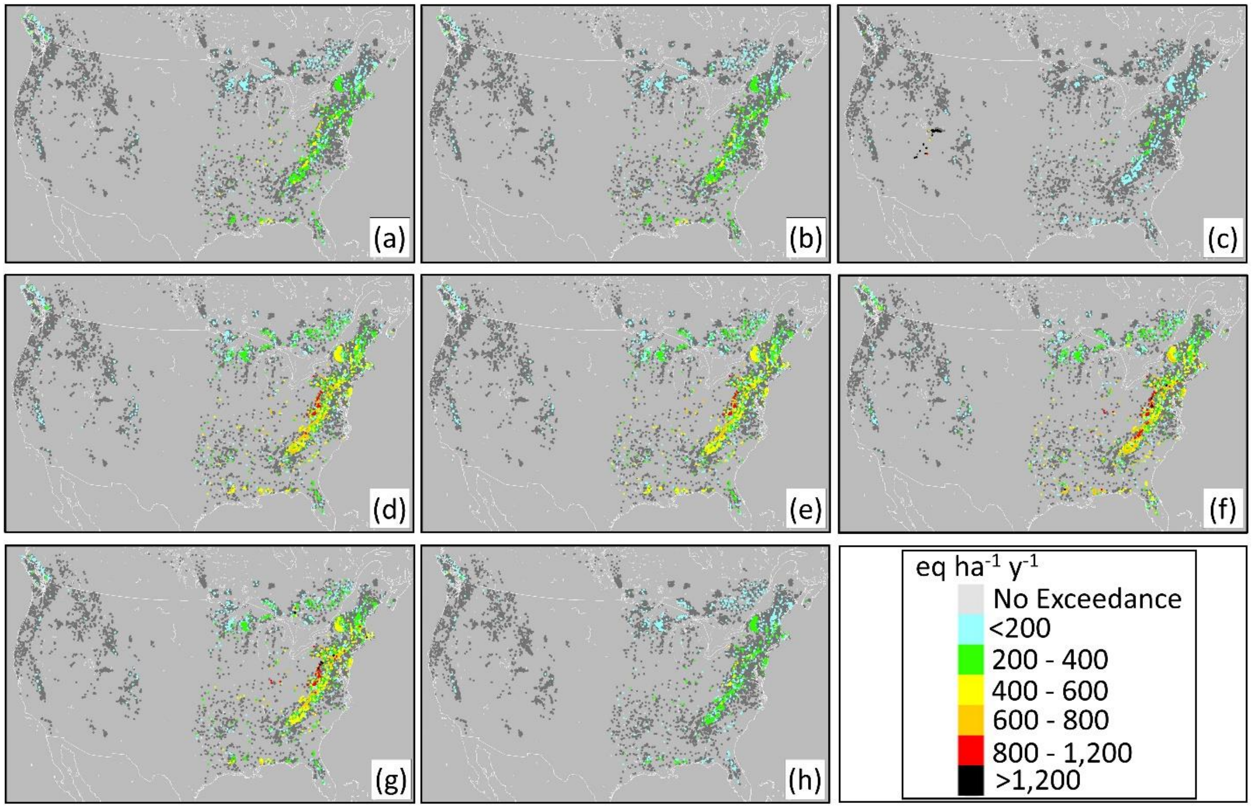

Figure S5. CLEs for Lichen Species, NA domain, 2010, eq ha^{-1}yr^{-1}. Panels arranged by model as in Figure S3. Light grey areas indicate regions for which critical load data were available but were not in exceedance of critical loads. Coloured areas indicate exceedance regions.

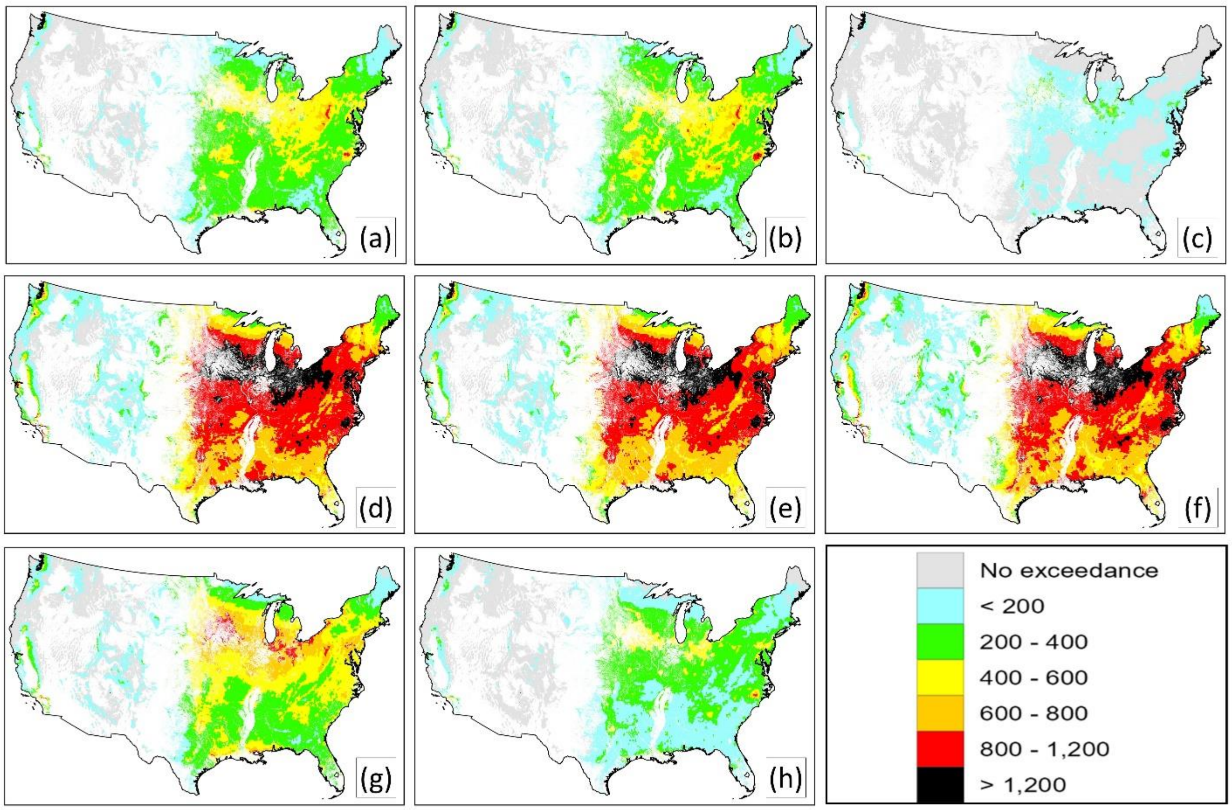

Figure S6. CLEs for Herbaceous Species Community Richness, NA common domain, 2010, eq ha^{-1}yr^{-1}. Panels arranged by mdel as in Figure S3. Light grey areas indicate regions for which critical load data were available but were not in exceedance of critical loads. Coloured areas indicate exceedance regions.

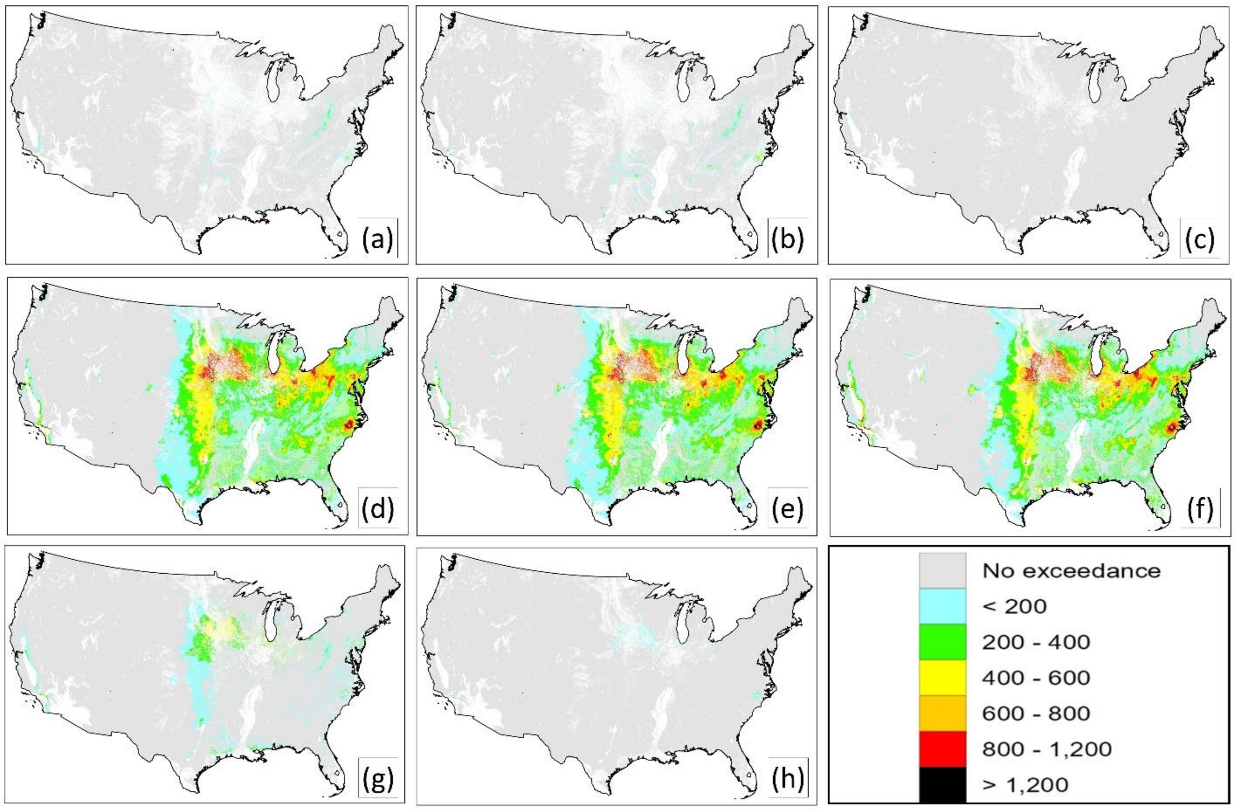

3.0 Observation Station Locations

Figure S7. (a) Wet S deposition station locations (yellow: CAPMoN daily wet deposition; green: NADP weekly wet deposition, (b) Daily PM2.5 sulphate and ammonium air concentration station locations.

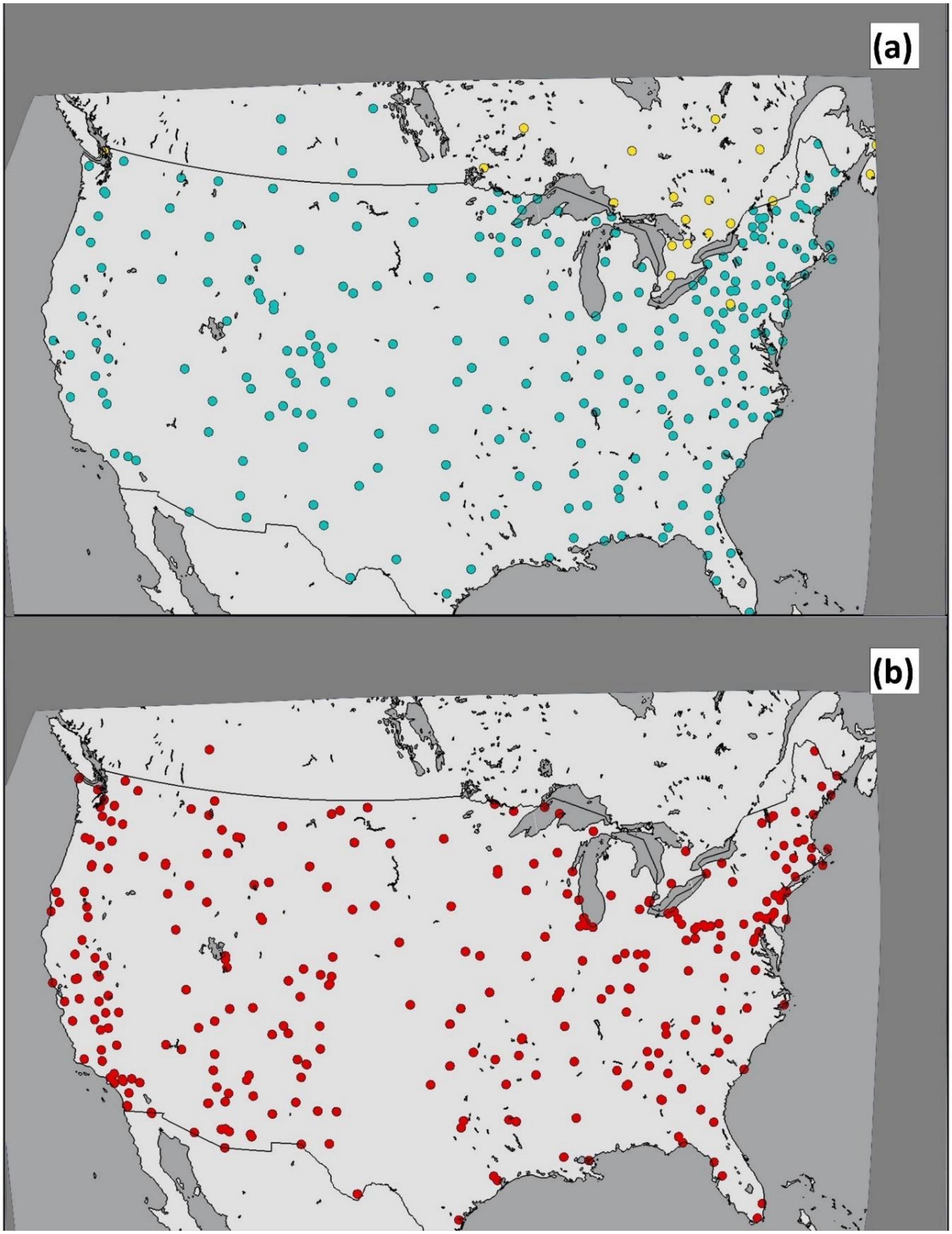

Figure S8. (a) SO_2 surface observation station locations (yellow: CAPMoN daily; yellow: NADP hourly green), (b) AMoN NH_3 Observation Stations, 2016.

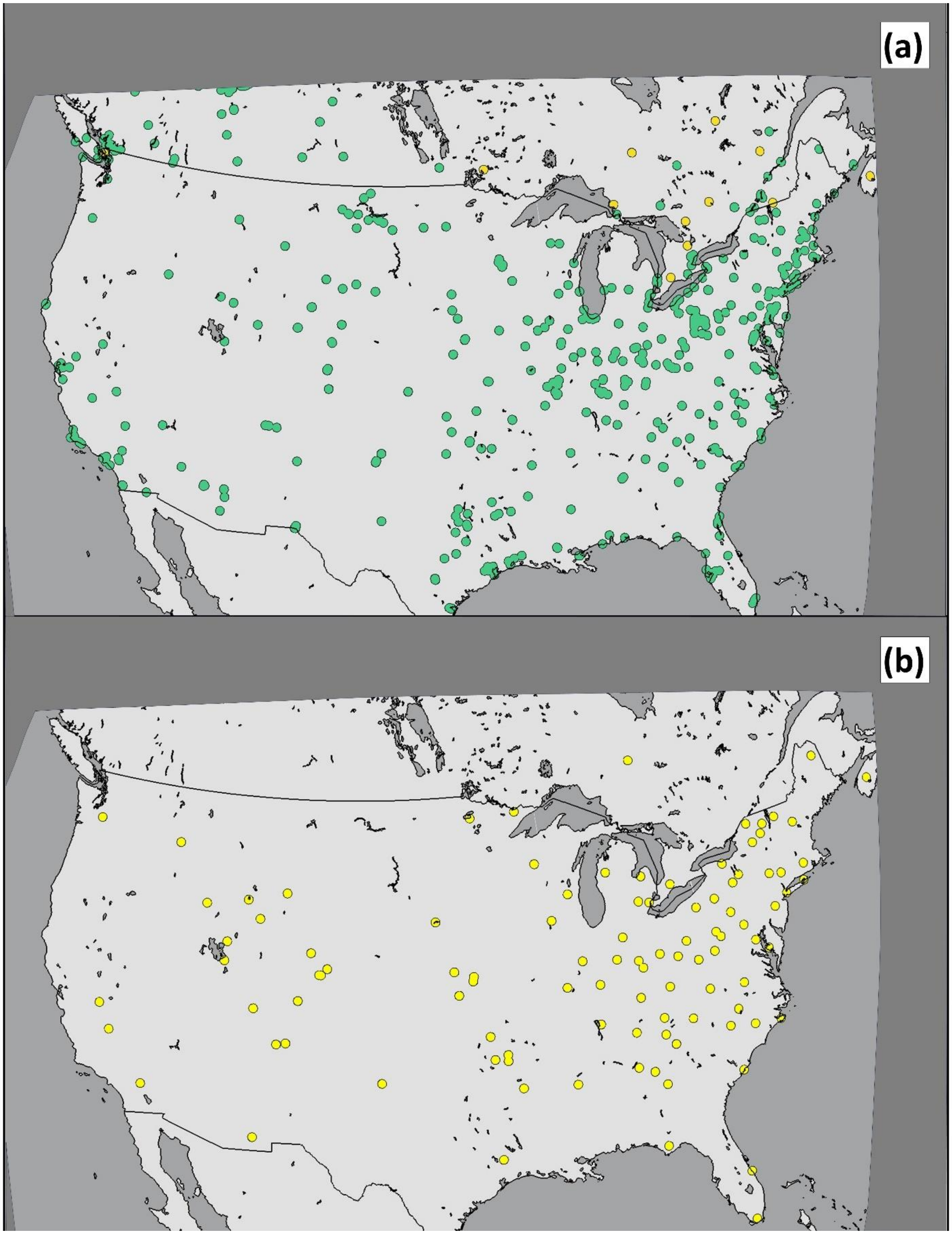

Figure S9. (a) SO_2 surface observation station locations (yellow: EMEP Hourly; green: AIRBASE hourly), and (b) EMEP wet deposition observation stations, EU AQMEII4 common domain, 2010.

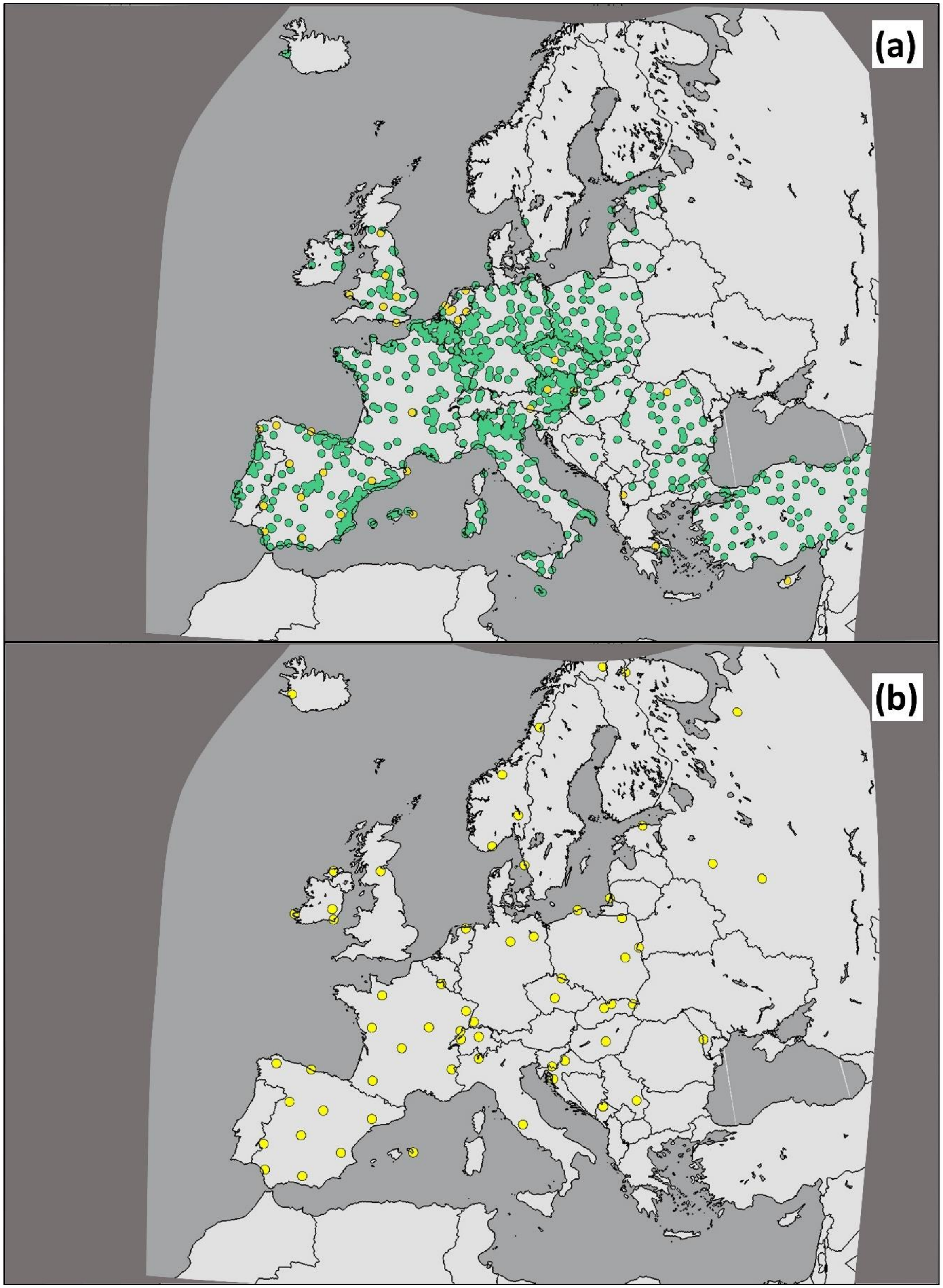

4.0 Cross-track Infrared Sounding (CrIS) Sensor Retrieval Details

The satellite surface volume mixing ratio ammonia observations are from the Cross-track Infrared Sounding (CrIS) sensor using the CrIS Fast Physical Retrieval (CFPR) algorithm (Shephard and Cady-Pereira, 2015; Shephard et al., 2020) with updates that include account for non-detects (White et al., 2023). The CrIS instrument pixel footprint is a 14 km circle at nadir with a 2200 km swath that provides complete daily global coverage. The CFPR minimum detection limit can vary depending on the atmospheric state but is as low as ~0.3-0.5 ppbv in favourable retrieval conditions (e.g. Kharol et al., 2018). In this study the CFPR 2016 pixel-level daytime observations, from NOAA/NASA Suomi National Polar-orbiting Partnership (SNPP) satellite over North America with a daytime local solar overpass time of 13:30, were gridded and averaged into annual values with a grid spacing of ~12.5 km to match up with model simulations.

References for CrIS section:

Kharol, S. K., Shephard, M.W., McLinden, C. A., Zhang, L., Sioris,C. E., O'Brien, J. M., Vet, R., Cady-Pereira, K. E., Hare, E.,Siemons, J., and Krotkov, N. A.: Dry deposition of reactive nitrogen from satellite observations of ammonia and nitrogen dioxide over North America, Geophys. Res. Lett., 45, 1157–1166, https://doi.org/10.1002/2017GL075832, 2018.

Shephard, M. W.; and Cady-Pereira, K. E.: Cross-track Infrared Sounder (CrIS) satellite observations of tropospheric ammonia, Atmos. Meas. Tech., 2015, 8, 1323–1336, https://doi:10.5194/amt-8-1323-2015.

Shephard, M. W.; Dammers, E.; Cady-Pereira, K. E.; Kharol, S. K.; Thompson, J.; Gainariu-Matz, Y.; Zhang, J.; McLinden, C. A.; Kovachik, A.; Moran, M.; Bittman, S.; Sioris, C.; Griffin, D.; Alvarado, M. J.; Lonsdale, C.; Savic-Jovcic, V.; and Zheng, Q.; Ammonia measurements from space with the Cross-track Infrared Sounder (CrIS): characteristics and applications, Atmos. Chem. Phys., 2020, 20, 2277–2302, https://doi.org/10.5194/acp-20-2277-2020.

White, E., M. W. Shephard, K. E. Cady-Pereira, S. Kharol, S. Ford, E. Dammers, E. Chow, N. Thiessen, D. Tobin, G. Quinn, J. O'Brien, J. Bash, Accounting for Non-detects in Satellite Retrievals: Application Using CrIS Ammonia Observations, Remote Sensing, 15, 2610, https://doi.org/10.3390/ rs15102610, 2023.

5.0 Precipitation Evaluation

Figure S10. Precipitation totals expressed as monthly averages, for (a) Daily NADP sites and (b) Weekly CAPMoN sites.

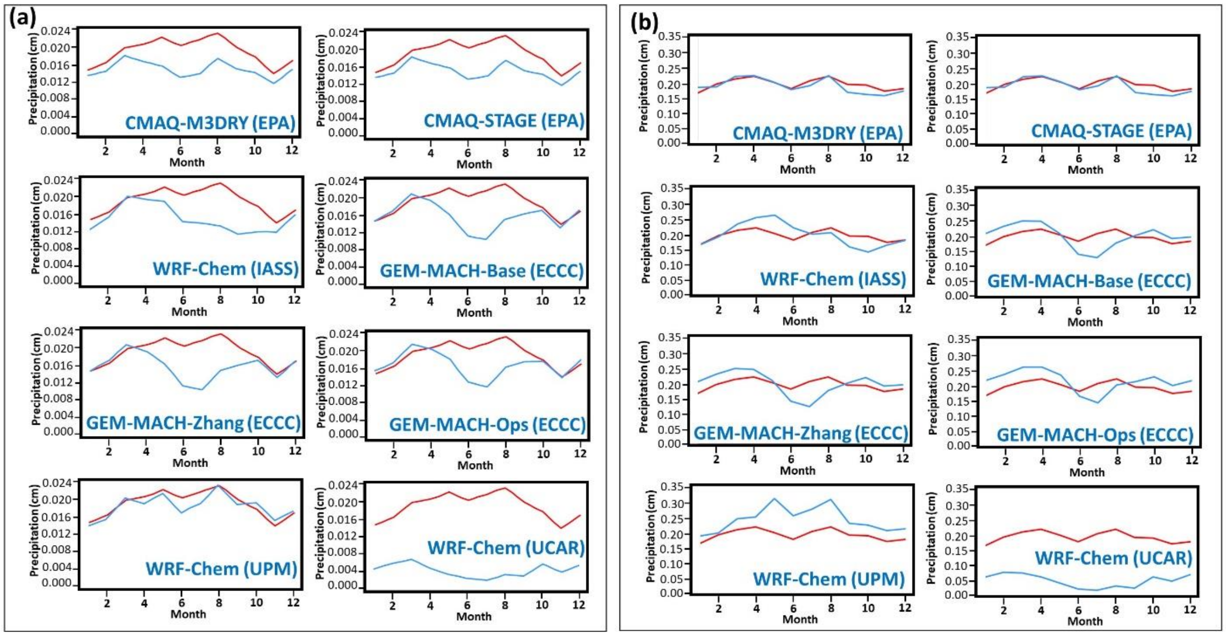

6.0 Additional annual effective mass flux figures

Figure S11. Spatial distribution of annual effective mass flux of HNO_3 via cuticle resistance pathway, AQMEII4 NA models, 2016 (eq ha^{-1} yr^{-1}).

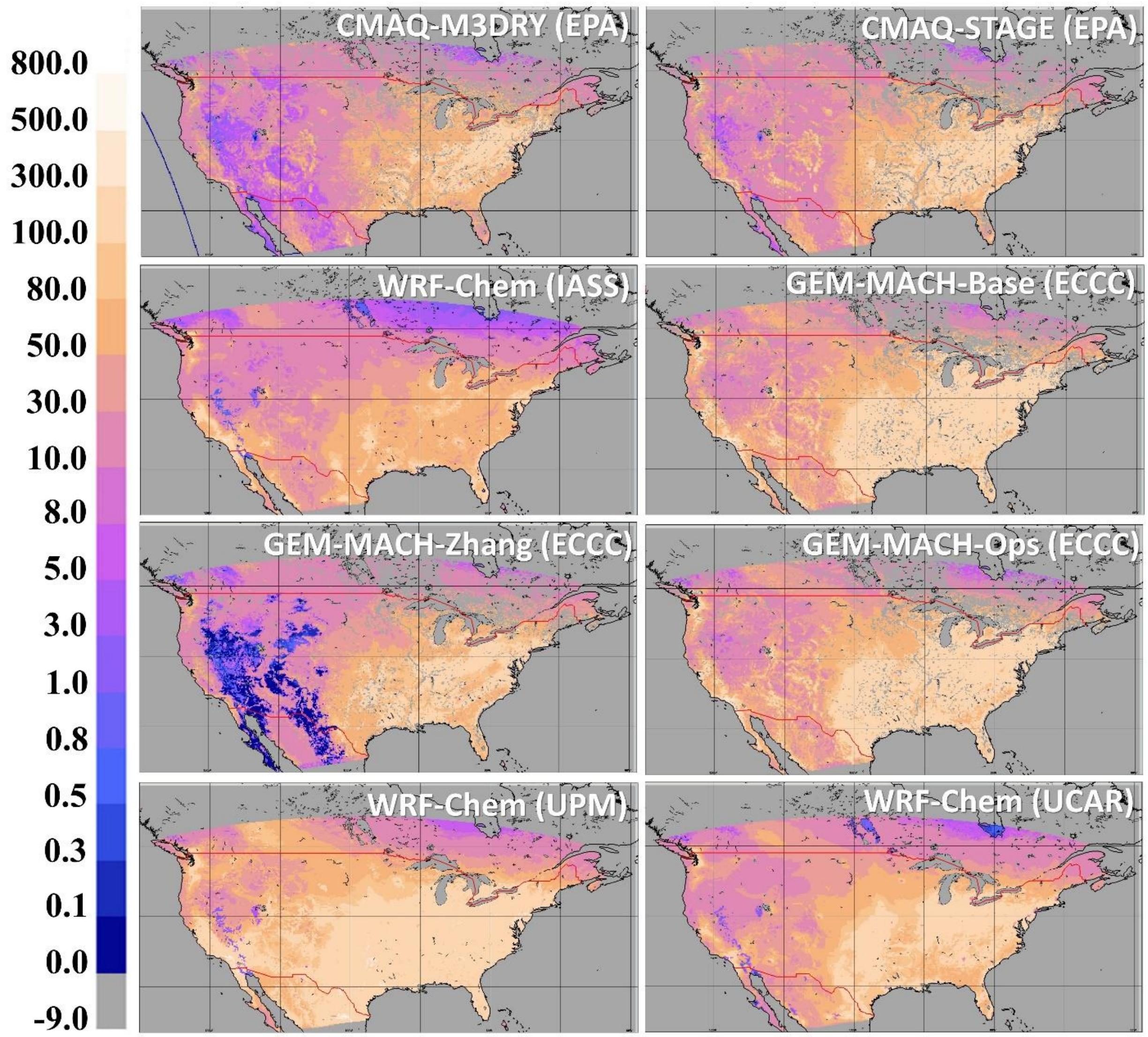

Figure S12. Spatial distribution of annual effective mass flux of HNO_3 via soil resistance pathway, AQMEII4 NA models, 2016 (eq ha^{-1} yr^{-1}). Note that the CMAQ models incorporate lower canopy effective flux as part of the soil effective flux (see Figure SI14).

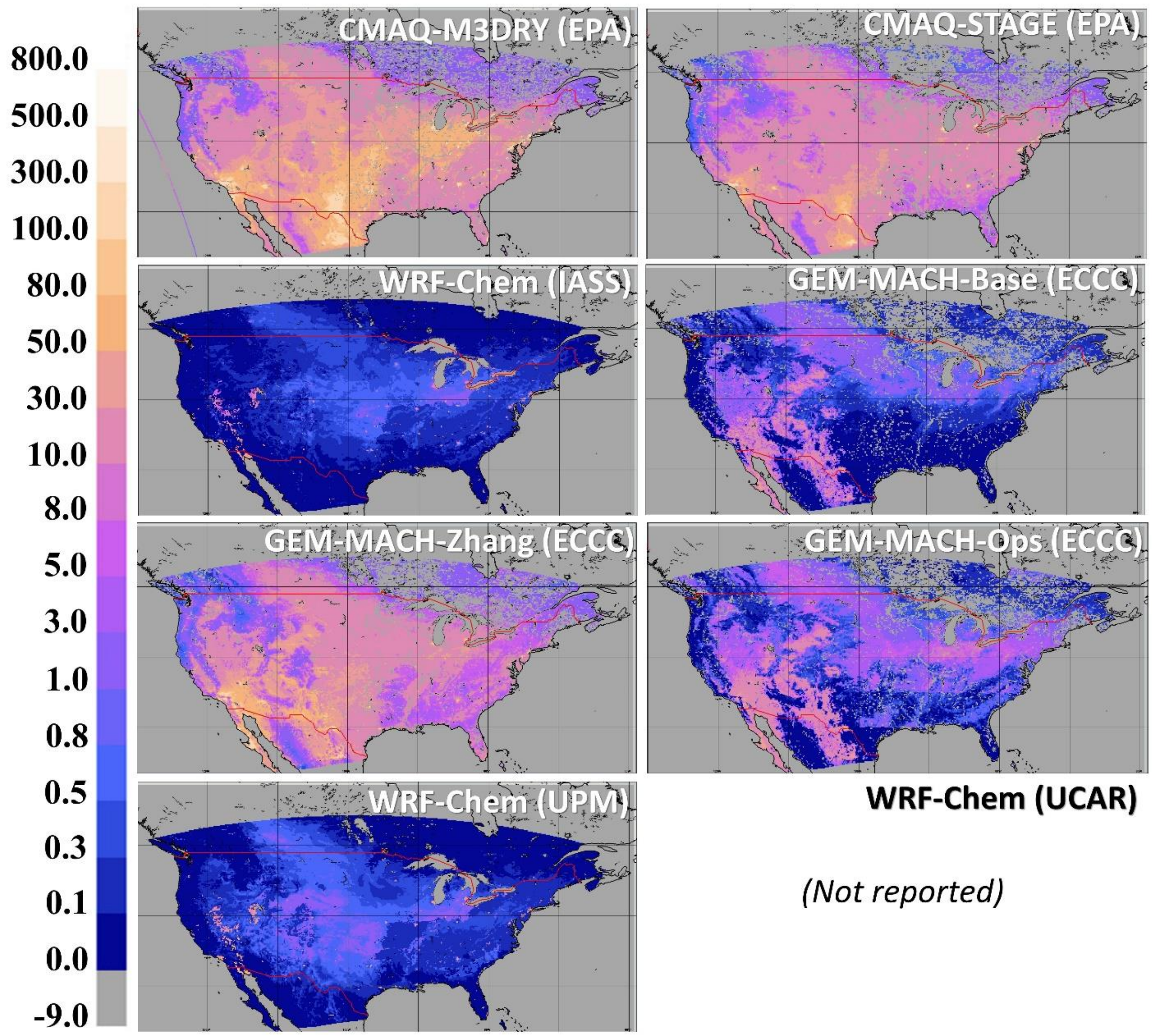

Figure S13. Spatial distribution of annual effective mass flux of HNO_3 via stomatal resistance pathway, AQMEII4 NA models, 2016 (eq ha^{-1} yr^{-1}).

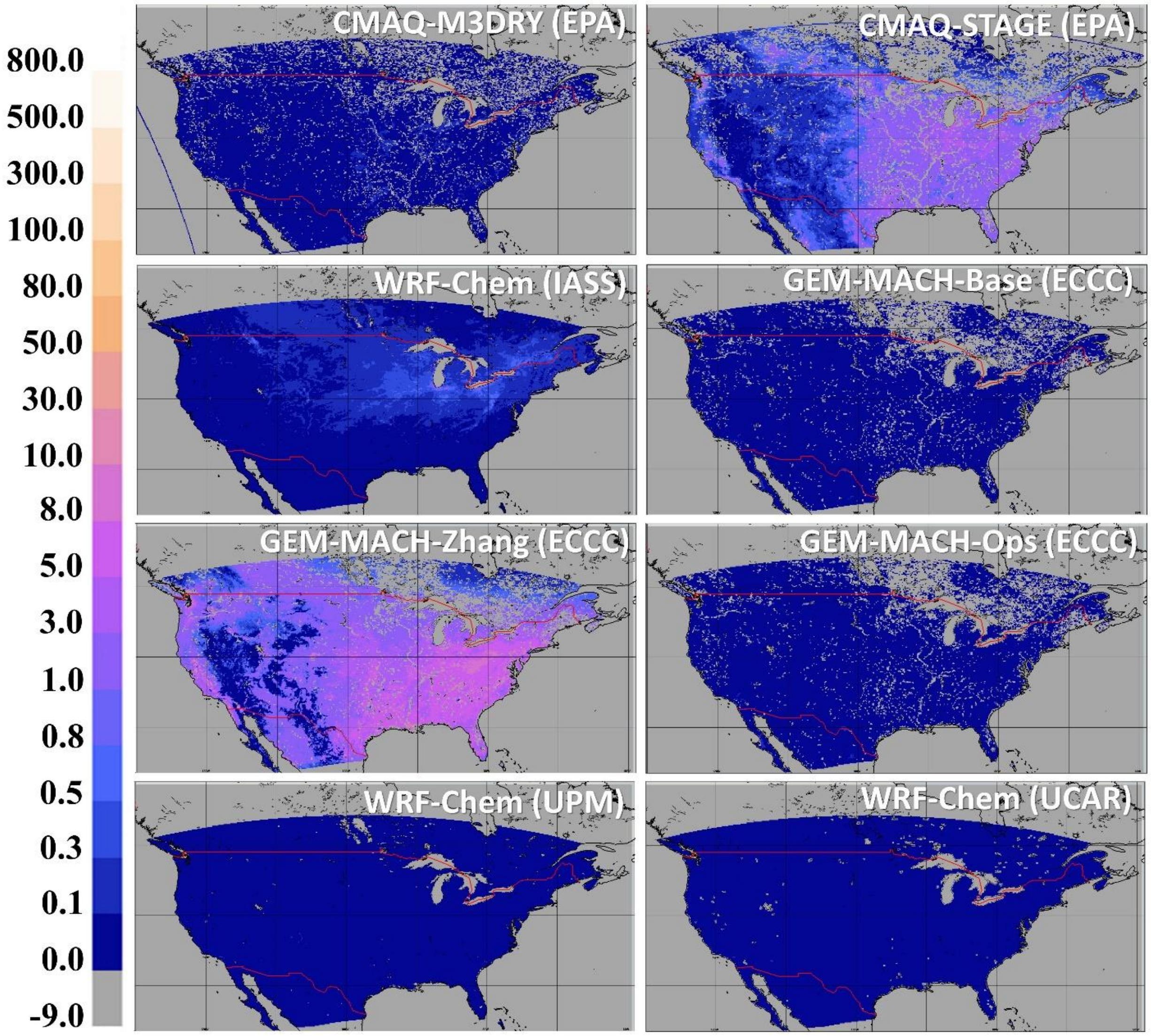

Figure S14. Spatial distribution of annual effective mass flux of HNO_3 via lower canopy resistance pathway, AQMEII4 NA models, 2016 (eq ha^{-1} yr^{-1}).

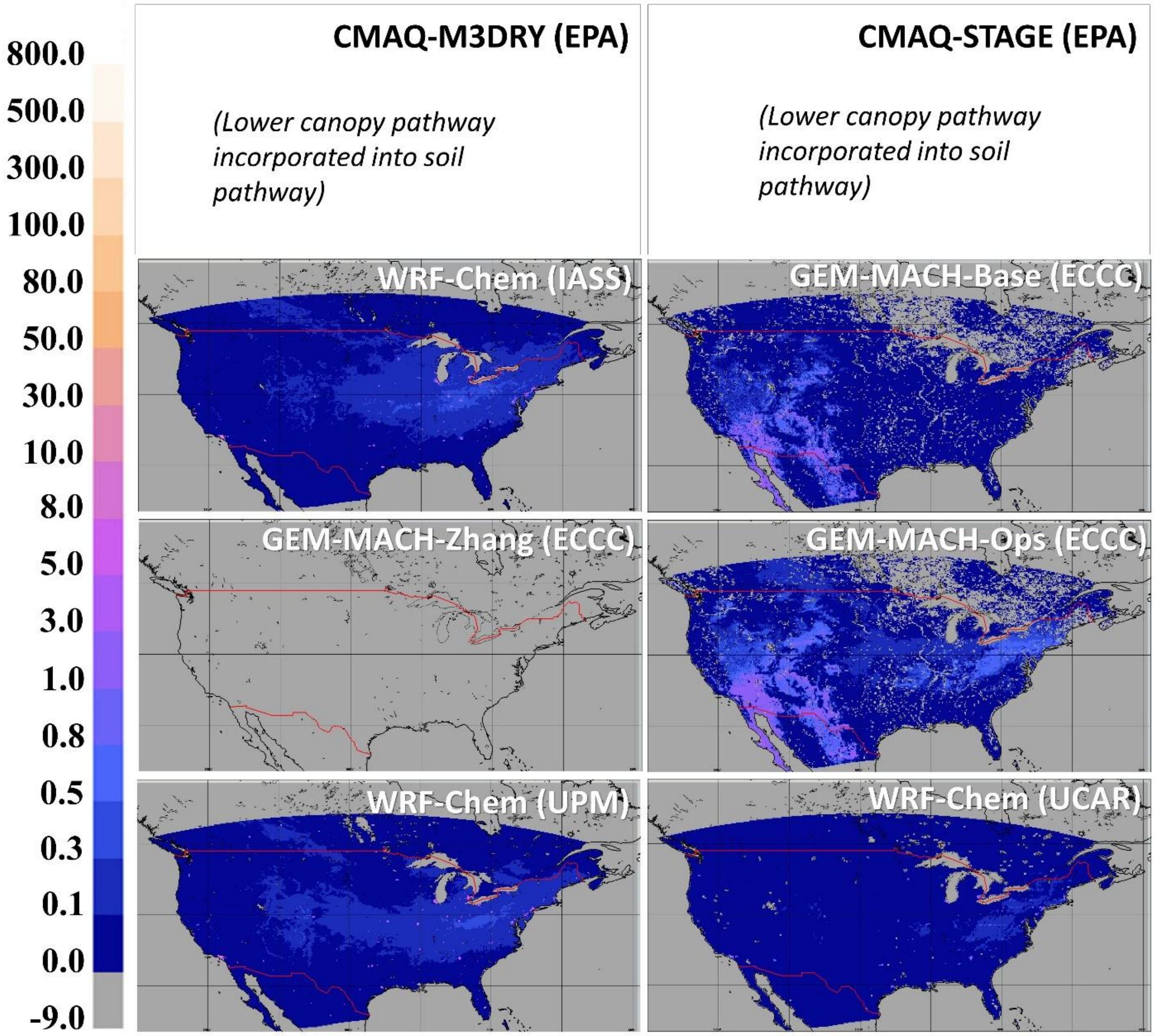

Figure S15. Spatial distribution of annual effective mass flux of SO_2 via cuticle (a) and (b) soil pathways, AQMEII4 EU models, 2010 (eq ha^{-1} yr^{-1}).

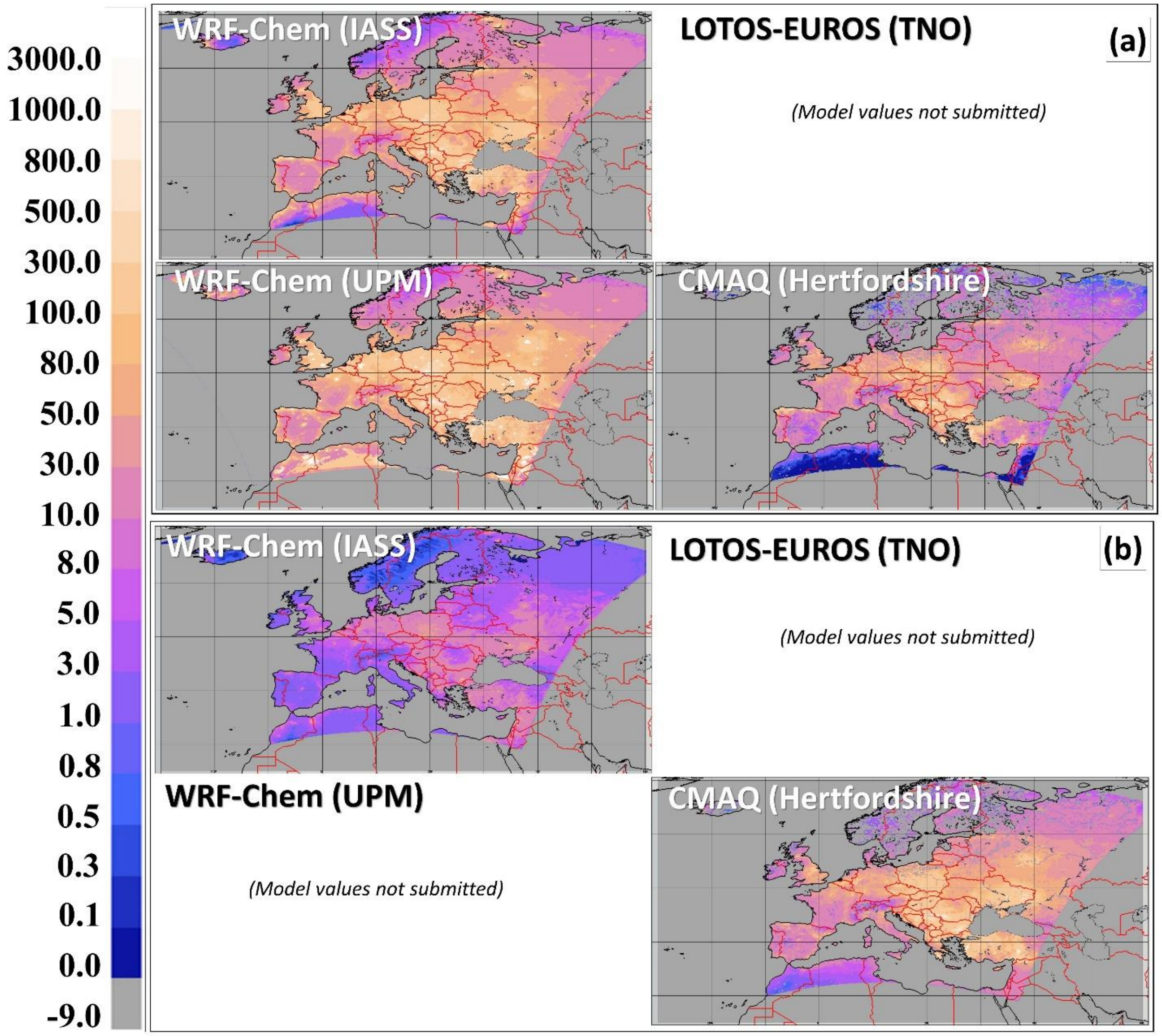

Figure S16. Spatial distribution of annual effective mass flux of SO_2 via stomatal (a) and (b) lower canopy pathways, AQMEII4 EU models, 2010 (eq ha^{-1} yr^{-1}).

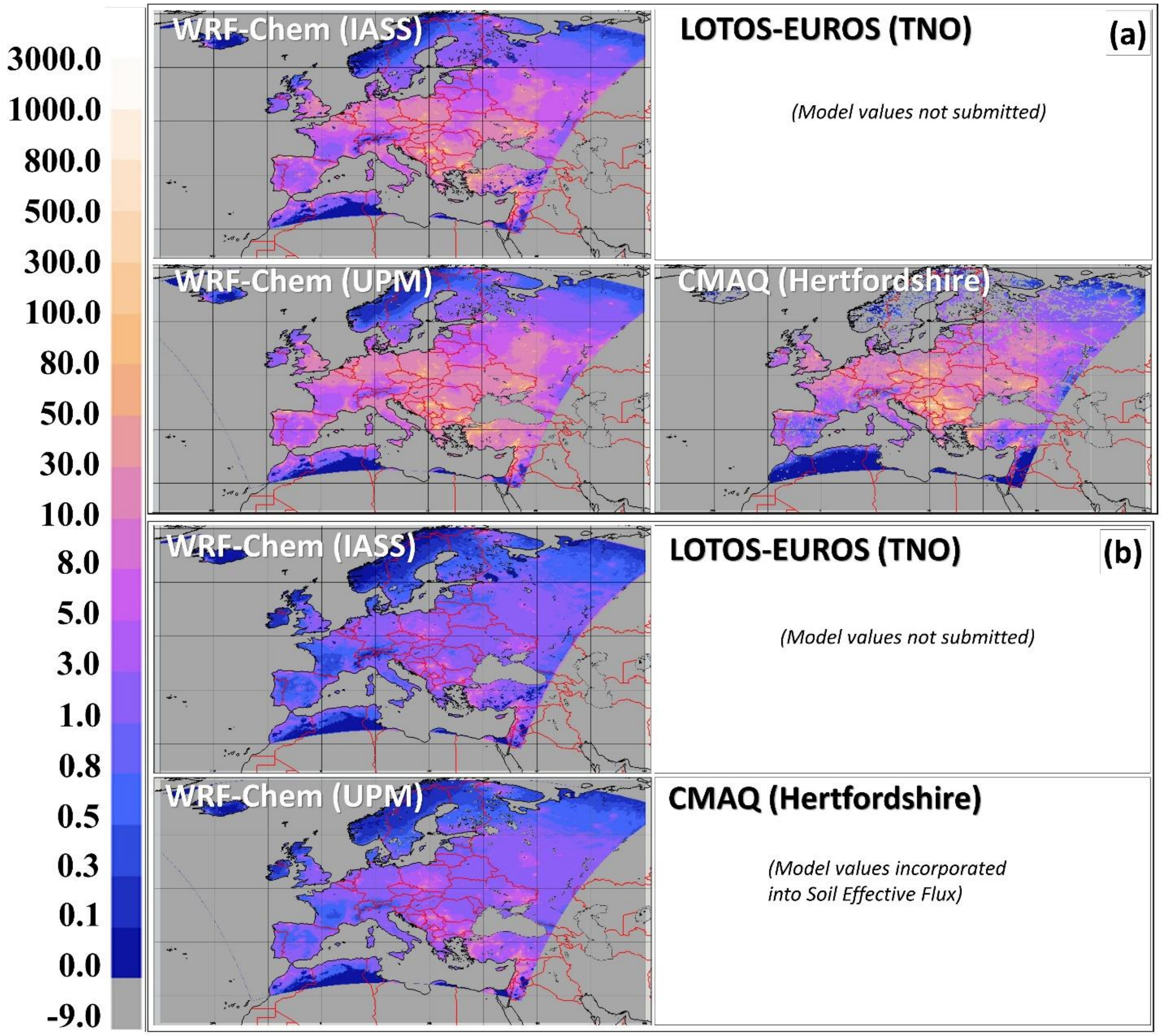

Figure S17. Spatial distribution of annual effective mass flux of HNO_3 via (a) cuticle, (b) soil pathways, AQMEII4 EU models, 2010 (eq ha^{-1} yr^{-1}).

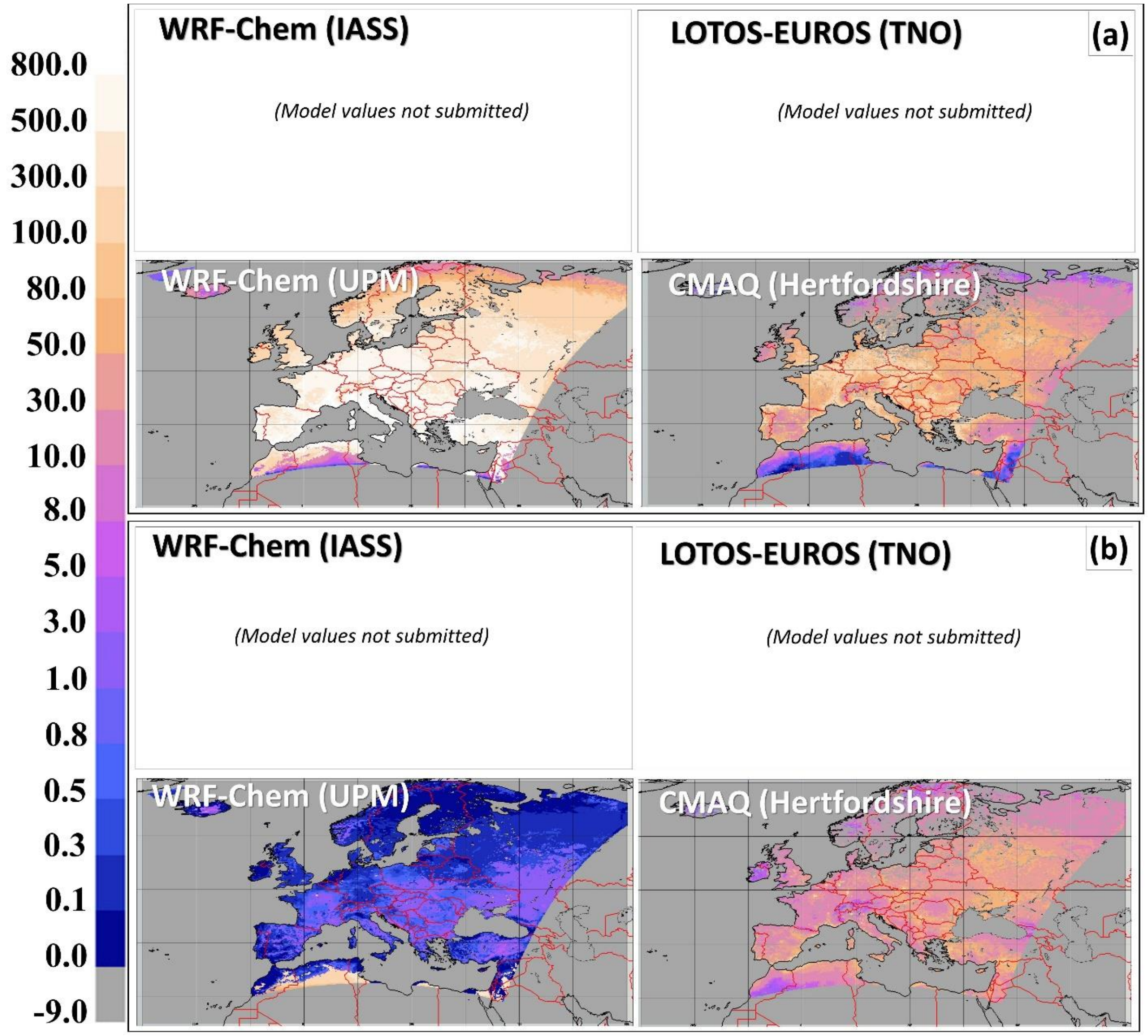

Figure S18. Spatial distribution of annual effective mass flux of HNO_3 via (a) stomatal resistance pathway, (b) lower canopy resistance pathway, AQMEII4 EU models, 2010 (eq ha^{-1} yr^{-1}).